energies

MDPI

Article

AC Voltage Control of DC/DC Converters Based on Modular Multilevel Converters in Multi-Terminal High-Voltage Direct Current Transmission Systems

Rui Li [1,*] and John E. Fletcher [2]

[1] Department of Electronic & Electrical Engineering, University of Strathclyde, Glasgow G1 1XW, UK
[2] School of Electrical Engineering and Telecommunications, University of New South Wales, Sydney 2052, Australia; john.fletcher@unsw.edu.au
* Correspondence: rui.li@strath.ac.uk; Tel.: +44-141-444-7331

Academic Editor: Gabriele Grandi
Received: 21 August 2016; Accepted: 8 December 2016; Published: 15 December 2016

Abstract: The AC voltage control of a DC/DC converter based on the modular multilevel converter (MMC) is considered under normal operation and during a local DC fault. By actively setting the AC voltage according to the two DC voltages of the DC/DC converter, the modulation index can be near unity, and the DC voltage is effectively utilized to output higher AC voltage. This significantly decreases submodule (SM) capacitance and conduction losses of the DC/DC converter, yielding reduced capital cost, volume, and higher efficiency. Additionally, the AC voltage is limited in the controllable range of both the MMCs in the DC/DC converter; thus, over-modulation and uncontrolled currents are actively avoided. The AC voltage control of the DC/DC converter during local DC faults, i.e., standby operation, is also proposed, where only the MMC connected on the faulty cable is blocked, while the other MMC remains operational with zero AC voltage output. Thus, the capacitor voltages can be regulated at the rated value and the decrease of the SM capacitor voltages after the blocking of the DC/DC converter is avoided. Moreover, the fault can still be isolated as quickly as the conventional approach, where both MMCs are blocked and the DC/DC converter is not exposed to the risk of overcurrent. The proposed AC voltage control strategy is assessed in a three-terminal high-voltage direct current (HVDC) system incorporating a DC/DC converter, and the simulation results confirm its feasibility.

Keywords: AC voltage control; DC/DC converter; DC fault protection; modular multilevel converter (MMC); multi-terminal high-voltage direct current (HVDC) system

1. Introduction

Due to the absence of common standards, current high-voltage direct current (HVDC) systems operate at different DC voltage levels. Similar to the AC transformer, the DC/DC converter can adapt a DC voltage to any higher or lower voltage level, which may be the only approach to connect and interconnect existing HVDC links operating at different DC voltages [1–3]. By blocking all the converters of the DC/DC converter, DC faults can be isolated without significantly affecting the healthy sections of the HVDC system. Additionally, the DC/DC converter can contribute to power flow and DC voltage control and can provide galvanic isolation for safety and system grounding reasons and for the normal operation of converters connected in a multi-terminal HVDC system [2,4].

The modular multilevel converter (MMC)-based DC/DC converter is an attractive approach in high voltage applications due to its modular design and relatively low switching losses [1,2,5] and thus is considered in this paper. The DC/DC converter proposed in [6] can isolate a DC fault quickly once the fault is detected. By utilizing two-level modulation with fundamental frequency, where

the AC voltage is clamped to plus or minus half the DC voltage, switching losses, submodule (SM) capacitance, and arm inductances are reduced. However, the electro-magnetic interference due to a rapid voltage change may be destructive.

A DC/DC converter with trapezoidal modulation is introduced in [2]. By blocking both MMCs in the DC/DC converter, a local DC fault, which occurs at the same branch as the DC/DC converter, can be isolated rapidly. The SM voltages are utilized to generate trapezoidal output voltages and reduce the dv/dt. However, the remote fault applied at the main HVDC link is not considered and it is a challenge to design the high voltage AC transformer for trapezoidal AC waveforms.

Besides the fast DC fault isolation capability, the DC/DC converter with sinusoidal modulation presented in [1,7] overcomes the EMI issue and simplifies the high voltage AC transformer design, which makes it preferred in HVDC applications.

Different modulation techniques are assessed in the referenced literature to improve the performance of the DC/DC converter with a focus on normal operation. During an AC fault, the half-bridge (HB)-based MMCs (HB-MMCs) still have full current control capability and do not suffer significant overcurrents. However, it is vulnerable to DC faults, where the fault currents flow through the antiparallel diodes from the AC side into the DC fault after the blocking of the MMC. The DC fault protection is thus considered in this paper. During a DC fault, all the HB-MMCs in the DC/DC converter have to be blocked to isolate the DC fault, as the adopted HB-MMCs do not have DC fault blocking capability.

The three-terminal DC/DC converter presented in [7] can isolate a fault by blocking only one MMC in the DC/DC converter while the other converters continue operating. However, the hybrid MMC is adopted to obtain DC fault blocking capability for each converter. Compared to a conventional DC/DC converter composed of HB-MMC, the capital cost, losses, and volume are increased making it undesirable for HVDC application.

Figure 1 shows a radial three-terminal HVDC system with a symmetric monopole structure, which is considered in this paper. Station S_3 with $\pm$300 kV DC voltage is connected to the main $\pm$400 kV HVDC link through a front-to-front DC/DC converter to match the different DC voltages and isolate any local fault on Cable 3. Stations S_1 and S_3 regulate the DC voltages of the DC network, while S_2 injects rated active power P_2 into the AC grid G_2. In the DC/DC converter, MMC_1 regulates the AC voltage, while MMC_2 operates in an active power control mode and exports rated power P_3 from the main DC-link to the AC-side. All the converters are modeled as conventional HB-MMCs using average models.

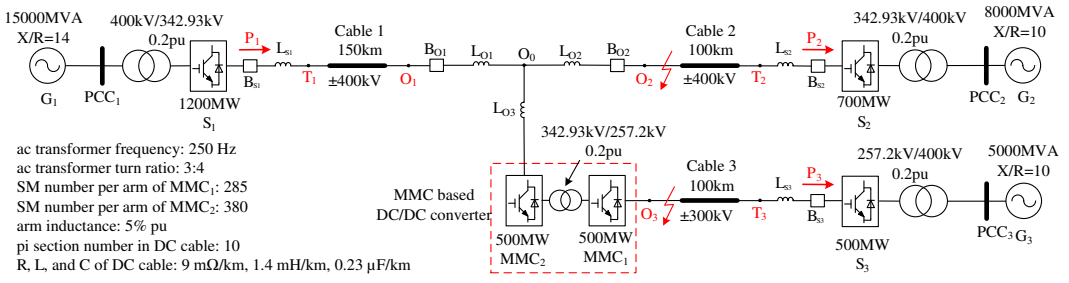

Figure 1. Radial three-terminal high-voltage direct current (HVDC) system using average models of half-bridge (HB)-based modular multilevel converters (MMCs), incorporating a front-to-front DC/DC converter based on MMCs.

If a DC fault occurs on Cable 2 (remote fault for the DC/DC converter), it is desirable that the DC/DC converter continues operating to maintain power transfer between stations S_1 and S_3, while the fault is isolated by the DC circuit breaker (DCCB) B_{O2} at the DC-link node. A mechanical DCCB in series with fault current limiting inductance is more likely to be used in a future super DC grid due to low conduction losses and capital cost [8,9]. However, the response of conventional mechanical circuit

breaker is slow, and the DC/DC converter still endures a high current stress during the response time. To avoid overcurrents in the DC/DC converter in continuous operation, active fault current control is proposed in [10]. However, the response of the DC/DC converter during a local fault on Cable 3 is not discussed.

For a local fault on Cable 3, the DC/DC converter is blocked to rapidly isolate the fault and operate stations S_1 and S_2 continuously. Conventionally, both the MMCs in the DC/DC converter are blocked [1,2,6]. This paper proposes standby operation of the DC/DC converter during a local fault, where only the MMC (MMC_1) connected to the faulty cable is blocked while the other MMC (MMC_2) continues operating and controls the AC voltage of the DC/DC converter at zero.

The main contribution of the paper is on the development of the improved AC voltage control strategy of the DC/DC converter, considering both normal operation and a local DC fault. In normal operation, the AC voltage is actively set according to the DC voltages of the converter to effectively utilize the DC voltage and generate higher output AC voltages. This significantly decreases SM capacitance and conduction losses of the DC/DC converter, yielding reduced capital cost, volume, and higher efficiency. Additionally, the standby operation during a local DC fault is proposed, where only the MMC connected to the faulty cable is blocked while the other MMC remains operational with zero AC voltage output. The proposed standby operation regulates the SM capacitor voltages at the rated value and avoids the decrease of the capacitor voltages after the blocking of the DC/DC converter. Moreover, the fault can still be isolated as quickly as the conventional approach, where both MMCs are blocked, and the DC/DC converter is not exposed to the risk of overcurrent.

This paper is organized as follows. The higher AC voltage operation of the DC/DC converter in normal operation is presented in Section 2. In Section 3, the influence of the increased AC voltage operation is addressed. Section 4 proposes standby operation of the DC/DC converter during a local DC fault. Performance of the proposed control strategy is assessed in Section 5. Section 6 draws conclusions.

2. Increased AC Voltage Operation of DC Transformer

The AC current, like the DC current, flows through MMC arm semiconductors. With increased AC voltages, the AC currents are correspondingly reduced to transfer rated power, yielding lower losses, especially conduction losses. Thus, MMCs are sensitive to AC voltage, which is preferably higher to reduce conduction losses and SM capacitances. However, the AC voltages need to be within the MMC output voltage capabilities to avoid over-modulation and ensure converter dynamics. When an MMC is a terminal station, the voltage of the AC grid connected to the MMC is allowed to fluctuate in the range of $\pm 10\%$ and thus the modulation index of the MMC terminal station is conventionally set between 0.75 and 0.85 [11,12]. Moreover, the AC voltage of the DC/DC converter is controllable and regulated by one MMC of the DC/DC converter. As a result, by properly setting the AC voltage of the DC/DC converter, the conduction losses can be significantly reduced while avoiding over-modulation [7].

In the presented increased AC voltage operation of the DC/DC converter, the modulation index is increased and can be set close to unity while avoiding over-modulation and retaining good dynamics. With a predefined higher modulation index, the AC voltages are determined by the DC voltages of the DC/DC converter, as shown in Figure 2. MMC_1 in the DC/DC converter operates in an AC voltage control mode and its control strategy is shown in Figure 2a, where PI control is used to accurately set the AC-side voltage of the DC/DC converter. The input voltage of the $dq/\alpha\beta$ block v_{dq1} is set by the AC voltage controller in normal operation and is switched to zero after a local DC fault is detected (i.e., standby operation, as will be discussed in Section 4). MMC_2 is assigned to control the active power with a control strategy illustrated in Figure 2b. Space vector (SV) modulation is used in both MMCs.

At the terminal stations, the q-axis component of the grid voltage is conventionally regulated at zero by a phase lock loop (PLL) [13]. Differently, as shown in Figure 2a, no PLL is required in MMC_1, which controls the AC voltage of the DC/DC converter. With the q-axis voltage reference set at zero

as illustrated in Figure 2, the d-axis voltage reference v_{d1ref} is set according to the two DC voltages of the DC/DC converter (v_{dc1} and v_{dc2}). The minimum of $m_{SV}v_{dc1}/\sqrt{3}$ and $m_{SV}nv_{dc2}/\sqrt{3}$ is the d-axis voltage reference:

$$v_{d1ref} = \frac{m_{SV}}{\sqrt{3}}\min(v_{dc1},\, nv_{dc2}) \tag{1}$$

where n is the AC transformer turn ratio, determined by the DC voltages of the DC/DC converter. By actively setting the AC voltage of the DC/DC converter according to Equation (1), the modulation index can be higher than the conventional approach [11,12] and the voltage generating capability of the DC/DC converter is effectively utilized to reduce conduction losses and SM capacitance, while the AC voltages are always within the converter control range, which avoids over-modulation and ensures good dynamics for the DC/DC converter. Considering the voltage drop on the inductances, the modulation index m_{SV} is lower than unity and is set at 0.95 in this paper. Even with such a high modulation index, the DC/DC converter still shows good dynamics during the studied fast power reversal process, as will be demonstrated in Section 5.

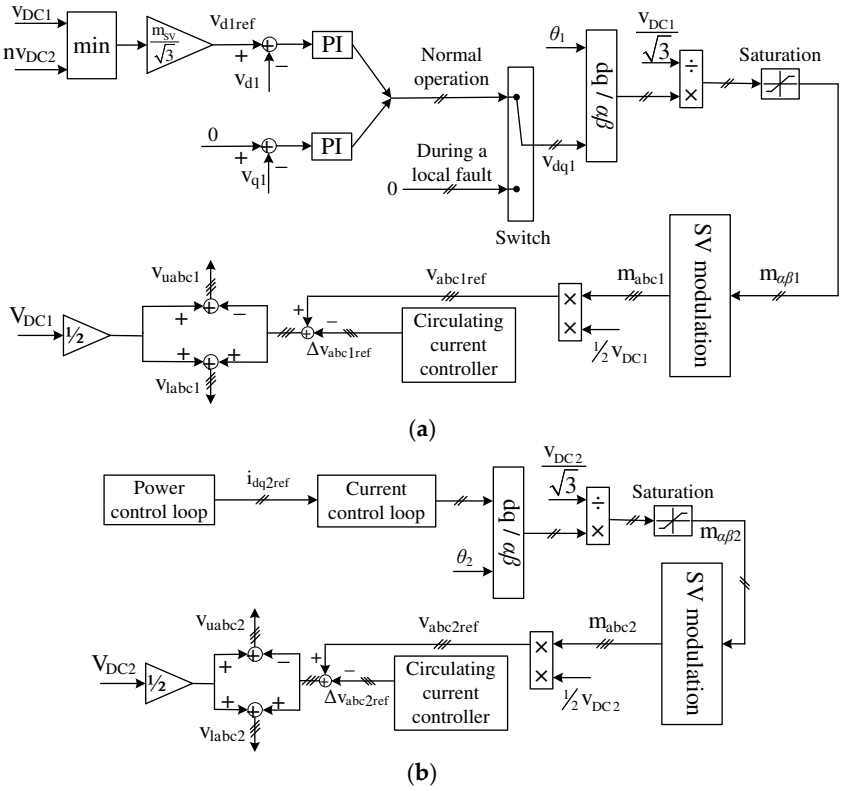

Figure 2. Proposed control strategy of the DC/DC converter: (**a**) AC voltage control; (**b**) power control. PI: Proportional–integral; SV: Space-vector.

At conventional MMC terminal stations with high AC voltage, the DC fault currents are higher due to the higher AC voltages. However, for the DC/DC converter, the fault currents can be suppressed to zero rapidly by the proposed standby operation as will be discussed in Section 4, even with increased AC voltages. As a result, increased AC voltage operation of the DC/DC converter has no adverse influence on DC fault currents. As the AC voltage is set by one MMC in the DC/DC converter and both MMCs operate with increased AC voltages, the turn ratio of the AC transformer, which is used for galvanic isolation and voltage matching, remains unchanged.

3. Influence of AC Voltage on the DC Transformer

The AC voltage influence on the DC/DC converter SM capacitance, conduction losses, and circulating currents are analyzed in this section.

3.1. Submodule (SM) Capacitance Requirements

Integrating the arm current multiplied by the arm voltage, the arm energy variation is derived as follows [14]:

$$\begin{array}{l}\Delta E_{arm} = \int_0^t v_{arm} i_{arm} \mathrm{d}t = \\ \frac{V_{dc} I_{dc}}{6\omega}\left\{-\frac{\sqrt{3}}{m_{SV}\cos\varphi}[\cos(\omega t-\varphi)-\cos\varphi]+\frac{2}{\sqrt{3}}m_{SV}[\cos\omega t-1]+\frac{1}{2\cos\varphi}[\sin(2\omega t-\varphi)+\sin\varphi]\right\}- \\ \frac{m_{hSV} V_{dc} I_{dc}}{3\sqrt{3}\omega}\left\{-\frac{\cos 3\omega t-1}{3}+\frac{\sqrt{3}}{2m_{SV}\cos\varphi}\left[\frac{1}{2}\sin(2\omega t+\varphi)-\frac{1}{4}\sin(4\omega t-\varphi)-\frac{3}{4}\sin\varphi\right]\right\}\end{array} \quad (2)$$

where i_{arm} is the arm current, respectively; I_{dc} is the rated DC current; ω is the AC-side angular frequency of the DC/DC converter; φ is the phase angle between the phase voltage and current; m_{SV} is the SV modulation index and defined as the ratio between the phase voltage peak and half of the rated DC voltage $\frac{1}{2}V_{dc}$; m_{hSV} is the ratio between the third harmonic voltage peak and $\frac{1}{2}V_{dc}$.

Although the two MMCs (MMC_1 and MMC_2 in Figure 1) have different DC voltages, DC currents, AC voltages, and AC currents, their arm energy variations are the same. The arm energy variation is decreased to 108.4 kJ by increasing the modulation index from 0.85 to 0.95. With a SM capacitor voltage ripple of $\pm 10\%$, the SM capacitance is proportional to the energy variation. Consequently, the SM capacitance is correspondingly reduced by 21.6% when utilizing the increased AC voltage operation.

From Equation (2), the energy variation per arm is inversely proportional to the AC-side angular frequency ω of the DC/DC converter. As a result, the SM capacitance is linearly reduced with increased ω, yielding lower volume and capital cost of the SMs, albeit higher switching losses. Therefore, the tradeoff must be considered carefully when tuning the AC-side frequency of the DC/DC converter. As the SM capacitance of MMC terminal stations usually meet the requirement of 30 to 40 kJ/MVA, as suggested by ASEA Brown Boveri (ABB) in [15], the SM capacitance correspondingly needs to be in the range of $\frac{30\omega_g}{\omega}$ to $\frac{40\omega_g}{\omega}$ kJ/MVA, where ω_g is the grid angular frequency.

3.2. Conduction Losses

Increased AC voltage operation cannot only reduce SM capacitance, but also lowers conduction losses. The conduction losses are significant for the MMC due to the large number of semiconductors in the current path and are considered in this section, although switching losses are similar for the different modulation methods being considered.

For simplicity, the forward voltages of the insulated-gate bipolar transistor (IGBT) and anti-parallel diode are assumed identical and denoted as V_{fd}. As the semiconductor number in the current path per arm is N, MMC conduction loss of the DC/DC converter can be approximated as follows [14]:

$$P_{loss} = \frac{6}{2\pi}\int_0^{2\pi} N V_{fd}|i_{arm}|\mathrm{d}(\omega t) = \frac{4NV_{fd}I_{dc}}{\pi}\left[\frac{\sqrt{3-(m_{SV}\cos\varphi)^2}}{m_{SV}\cos\varphi}+\arccos\sqrt{1-\frac{(m_{SV}\cos\varphi)^2}{3}}\right] \quad (3)$$

By increasing the modulation index from 0.85 to 0.95, the conduction losses of the DC/DC converter are reduced by 8.1%, yielding higher efficiency and a reduced cooling requirement.

3.3. Circulating Voltages

The circulating current is generated by the circulating voltage, which is imposed on the upper and lower arm inductors and is proportional to the phase energy variation ΔE_p [14]. ΔE_p is the sum of the upper and lower arm voltages (ΔE_u and ΔE_l, respectively), as depicted by Equation (4):

$$\begin{array}{l}\Delta E_p = \Delta E_u + \Delta E_l \\ = \frac{V_{dc} I_{dc}}{6\omega\cos\varphi}[\sin(2\omega t-\varphi)+\sin\varphi]-\frac{m_{hSV} V_{dc} I_{dc}}{3m_{SV}\omega\cos\varphi}\left[\frac{1}{2}\sin(2\omega t+\varphi)-\frac{1}{4}\sin(4\omega t-\varphi)-\frac{3}{4}\sin\varphi\right]\end{array} \quad (4)$$

As the ratio between MMC modulation index m_{SV} and third harmonic voltage modulation index m_{hSV} is fixed, increasing the modulation index has no influence on the phase energy variation and only the third harmonic contributes to phase energy variation reduction.

4. Standby Operation of the DC/DC Converter during a Local Fault

Although SM capacitor discharge through a DC fault path can be avoided by blocking the MMC, the energy stored on the SM capacitors is dissipated slowly due to the non-ideal behaviors of devices in practice, such as the capacitor leakage, the equivalent series resistance (ESR), the wiring resistance, and the collector-emitter cutoff current of IGBT I_{CES}. This causes a SM voltage decrease. As I_{CES} and the parasitic resistances are usually small, the SM voltage decrease is slight if the converter blocking time is short.

If the fault lasts long enough, the SM voltages will decrease to a value much lower than rated and will drop to zero eventually. In this condition, after the fault is cleared, the SM capacitors must be charged back to around the rated value as suggested in [16,17], and the MMC can then be restarted.

Conventionally, both the MMCs in the DC/DC converter are blocked to isolate a local fault from the healthy sections of the HVDC system. However, it was found in this work that it is unnecessary to block both MMCs in the DC/DC converter during a DC fault. The standby operation of the DC/DC converter during a local fault is thus proposed, where only the MMC (MMC_1) connecting to the faulty cable needs to be blocked, while the other MMC (MMC_2) continues operating and controls the AC voltage of the DC/DC converter at zero. As illustrated in Figure 2a, the input voltage of the $dq/\alpha\beta$ block v_{dq1} is switched to zero after a local DC fault is detected. This yields a zero modulation index, and the output voltage v_{abc1} is correspondingly controlled around zero, as displayed in Figure 3. As a result, the SM capacitor voltages of MMC_2 remain at the rated value and the decrease of the SM capacitor voltages after the blocking of the DC/DC converter is avoided. Moreover, the fault can still be isolated as quickly as the conventional approach, where both MMCs are blocked, and the DC/DC converter is not exposed to the risk of overcurrent. The standby operation of the DC/DC converter is a specific application of the proposed AC voltage control during a local DC fault.

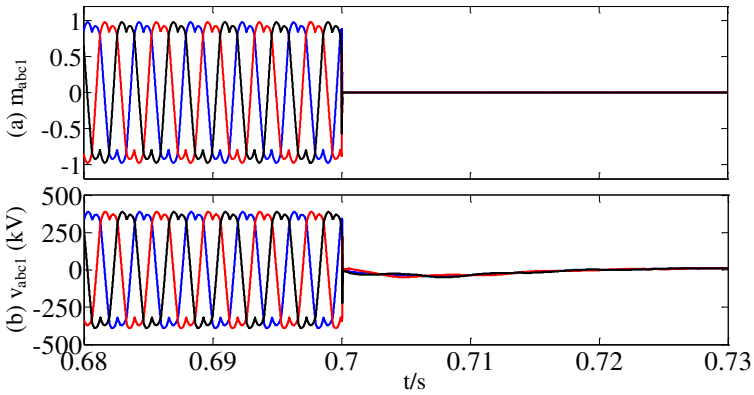

Figure 3. AC quantities of the DC/DC converter in the proposed standby operation in the event of a local DC fault at t_0 = 0.7 s: (**a**) three-phase modulation waveforms; and (**b**) three-phase output voltages.

The proposed scheme is relatively independent on the fault detection time, which is assumed at 1 ms in this paper [18]. After a local DC fault occurs at t_0 = 0.7 s, MMC_1 is blocked and MMC_2 is switched to AC voltage control mode at t_0 = 0.701 s. As the DC voltage of MMC_1 drops to zero due to the pole-to-pole DC fault, the AC voltage reference of MMC_2 is set to zero to avoid the fault currents flowing from the AC-side to the DC-side in MMC_1. For MMC_2, as the AC output voltage v_{AC} is zero, all the arm voltages v_{arm} are controlled at half the rated DC voltage V_{dc}:

$$v_{arm} = \frac{1}{2}V_{dc} - v_{ac} = v_{ac} - \left(-\frac{1}{2}V_{dc}\right) = \frac{1}{2}V_{dc}. \quad (5)$$

Thus, half the SM capacitors are connected in the current path in each arm while the other (half) SM capacitors are bypassed:

$$N_i = N_b = \frac{1}{2}N \quad (6)$$

where N, N_i, and N_b are the total, inserted, and bypassed SMs per arm.

By using voltage balance control, all the SM capacitor voltages of MMC_2 are controlled around their rated value. After the fault is cleared, the AC voltage of the DC/DC converter can be restored quickly, benefiting from the stored SM capacitor energy of MMC_2. As a result, the SM capacitors of MMC_1 can be charged by the AC voltages to quickly restore the operation of the DC/DC converter. Fast restart capability is thus achieved by standby operation of the DC/DC converter.

As shown in Figure 4a, MMC_2 remains operational and the sum of the SM capacitor voltages per arm is well regulated at the rated value (800 kV) with limited overshoot, after a DC fault occurs at t_0 = 0.7 s. The converter arm currents are fully controlled and decay to around zero (Figure 4c). Although MMC_2 continues operation, the fault can still be blocked due to the zero AC voltage regulated by MMC_2. The arm currents of MMC_1 briefly exhibit fault currents as the DC cable capacitance discharges during the initial period of the DC fault and then decrease to zero (Figure 4d).

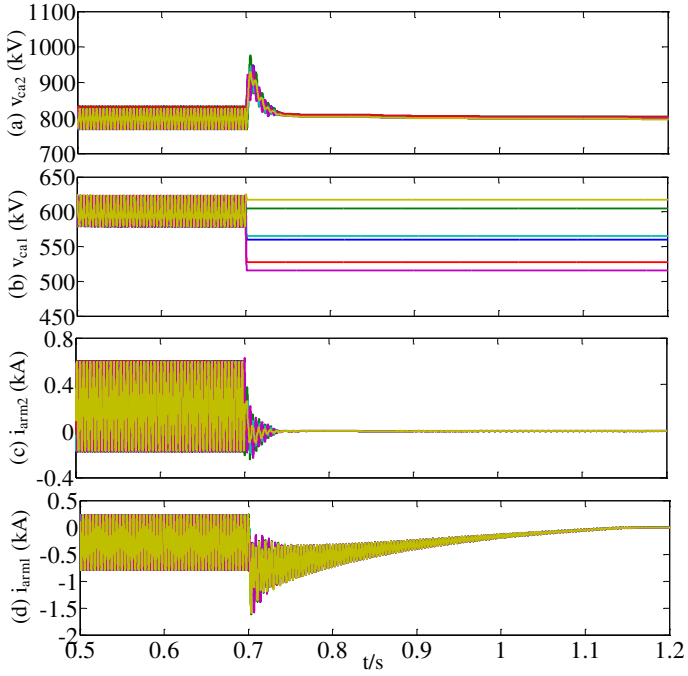

Figure 4. Other waveforms in the proposed standby operation of the DC/DC converter during a fault on Cable 3 at t_0 = 0.7 s: (**a**) sum of the SM capacitor voltages per arm of MMC_2; (**b**) the sum of the SM capacitor voltages per arm of MMC_1; (**c**) arm currents of MMC_2; and (**d**) arm currents of MMC_1.

5. Power Reversal Performance of the AC Voltage Control Strategy

Higher output voltage is required for the MMCs in the DC/DC converter to quickly reverse power. However, due to the voltage drop on the DC cables, the DC voltage of the DC/DC converter is potentially lower than the rated value. Additionally, one of the two DC voltages of the DC/DC converter increases during power reversal while the other drops. Fast power reversals place an onerous requirement for the voltage generating capability of the MMC to avoid over-modulation and uncontrolled AC currents in the proposed increased AC voltage operation, where the modulation index is close to unity.

To assess the performance of the AC voltage control strategy during power reversal operation, the simulated scenario assumes MMC_1 in Figure 1 is initially commanded to import 500 MW from the main DC-link to the grid G_3, then the power flow direction is reversed at time t = 0.8 s to export 500 MW from G_3 to the main DC-link. The rate of change of active power is restrained to 5 MW/ms and the modulation index is fixed at 0.95.

Figures 5 and 6 show waveforms during power reversal of the test system in Figure 1 under the mentioned operating conditions. In Figure 5b, limited DC voltage drop is observed by MMC_1. This results in over-modulation and uncontrolled AC currents due to high modulation index 0.95, if the AC voltage remains unchanged during power reversal. To overcome this issue, the AC voltage of the DC/DC converter is actively set according to the two DC voltages, as previous mentioned. As a result, the AC voltage dips in Figure 5a following the DC voltage

drop of MMC_1 during the power reversal. Thus over-modulation and uncontrolled AC currents are actively avoided, while the AC voltage is controlled as high as possible to reduce conduction losses and SM capacitance.

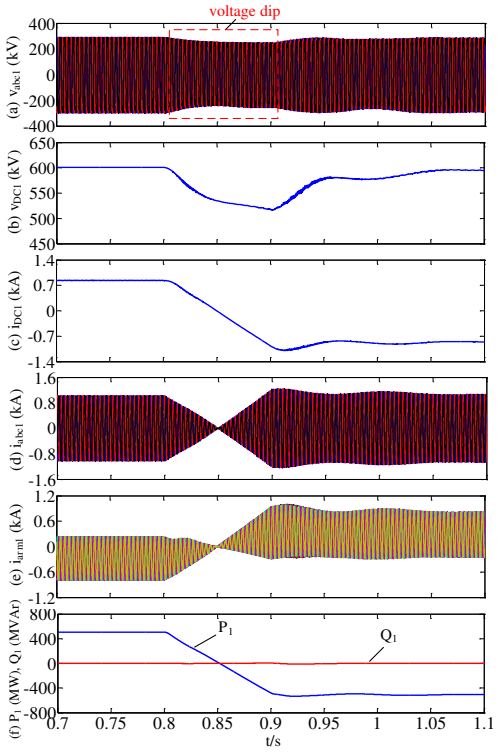

Figure 5. Power reversal waveforms of MMC_1 in the DC/DC converter: (**a**) three-phase voltages; (**b**) DC voltage; (**c**) DC current; (**d**) three-phase currents; (**e**) arm currents; and (**f**) active and reactive powers.

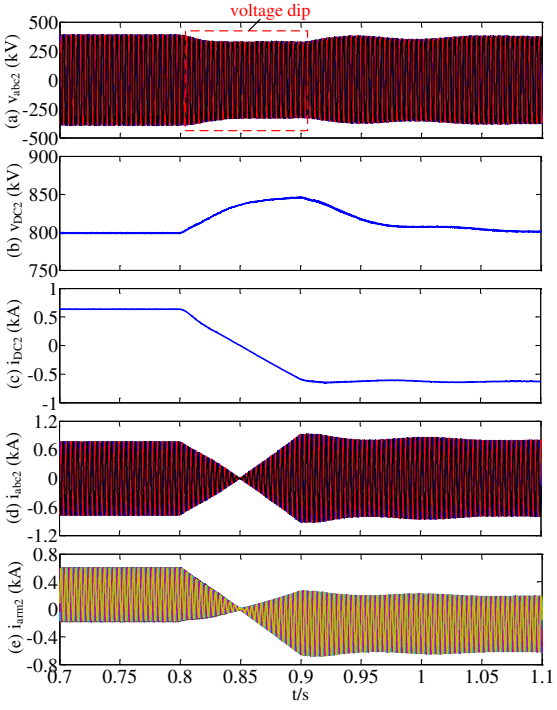

Figure 6. Power reversal waveforms of MMC_2 in the DC/DC converter: (**a**) three-phase voltages; (**b**) DC voltage; (**c**) DC current; (**d**) three-phase currents; and (**e**) arm currents.

Power reversal is achieved with minimal transient effects in the AC currents and the active and reactive powers of MMC_1 (a converter that regulates AC voltage level) (Figure 5d,f), as is also the case for MMC_2 (a converter that regulates active power). During active power reversal, as commanded by MMC_2, DC current reverses in both HVDC links, with limited overshoot due to the dynamics associated with the loop inductances of the link (arm and DC cables). The arm currents of MMC_1 and MMC_2 reverse with slight overshoot during power reversal operation, as shown in Figures 5e and 6e. Following power reversal, the HVDC transmission system reaches its steady state operating point. The results in Figures 5 and 6 show that the DC/DC converter with increased AC voltage operation is able to operate over the entire operating range, with voltage and current stresses in the active and passive devices fully controlled.

6. Conclusions

In the proposed AC voltage control strategy, the modulation index can be higher than conventional approaches and the voltage generating capability of the MMC is effectively utilized by actively setting the AC voltage according to the two DC voltages of the DC/DC converter. Over-modulation and uncontrolled currents are actively avoided by limiting the AC voltage in the controllable range of both MMCs in the DC/DC converter. The SM capacitance and conduction losses are significantly reduced, yielding lower capital cost and volume, and increased efficiency.

Standby operation of the DC/DC converter during a local DC fault is proposed, where only the MMC connected on the faulty cable is blocked while the other MMC remains operational with zero AC voltage output. Thus, the SM capacitor voltages can be controlled at the rated voltage, and the capacitor voltage dropping after the blocking of the converter is avoided. Moreover, the fault can still be isolated as quickly as the conventional approach, where both MMCs are blocked, and the DC/DC converter is not exposed to the risk of overcurrent.

Author Contributions: Both authors were involved during the development of the manuscript. Rui Li wrote the paper and was in charge of most of the modeling. John E. Fletcher provided valuable insights throughout the research and writing processes.

Conflicts of Interest: The authors declare no conflict of interest.

References

1. Kenzelmann, S.; Rufer, A.; Vasiladiotis, M.; Dujic, D.; Canales, F.; de Novaes, Y.R. A versatile DC-DC converter for energy collection and distribution using the Modular Multilevel Converter. In Proceedings of the 2011—14th European Conference on Power Electronics and Applications (EPE 2011), Birmingham, UK, 30 August–1 September 2011.
2. Gowaid, I.A.; Adam, G.P.; Massoud, A.M.; Ahmed, S.; Holliday, D.; Williams, B.W. Quasi Two-Level Operation of Modular Multilevel Converter for Use in a High-Power DC Transformer with DC Fault Isolation Capability. *IEEE Trans. Power Electron.* **2015**, *30*, 108–123. [CrossRef]
3. Yong, L.; Longfu, L.; Rehtanz, C.; Can, W.; Ruberg, S. Simulation of the Electromagnetic Response Characteristic of an Inductively Filtered HVDC Converter Transformer Using Field-Circuit Coupling. *IEEE Trans. Ind. Electron.* **2012**, *59*, 4020–4031.
4. Jovcic, D. Bidirectional, High-Power DC Transformer. *IEEE Trans. Power Deliv.* **2009**, *24*, 2276–2283. [CrossRef]
5. Antonopoulos, A.; Angquist, L.; Harnefors, L.; Ilves, K.; Nee, H.P. Global Asymptotic Stability of Modular Multilevel Converters. *IEEE Trans. Ind. Electron.* **2014**, *61*, 603–612. [CrossRef]
6. Kenzelmann, S.; Rufer, A.; Dujic, D.; Canales, F.; de Novaes, Y.R. Isolated DC/DC Structure Based on Modular Multilevel Converter. *IEEE Trans. Power Electron.* **2015**, *30*, 89–98. [CrossRef]
7. Zeng, R.; Xu, L.; Yao, L. DC/DC Converters Based on Hybrid MMC for HVDC Grid Interconnection. In Proceedings of the 11th IET International Conference on AC and DC Power Transmission, Birmingham, UK, 10–12 February 2015.
8. Li, R.; Xu, L.; Holliday, D.; Page, F.; Finney, S.J.; Williams, B.W. Continuous Operation of Radial Multiterminal HVDC Systems Under DC Fault. *IEEE Trans. Power Deliv.* **2016**, *31*, 351–361. [CrossRef]
9. Wang, J.; Berggren, B.; Linden, K.; Pan, J. Multi-terminal DC system line protection requirement and high speed protection solutions. In Proceedings of the 2015 CIGRE Symposium, Cape Town, South Africa, 26–30 October 2015.

10. Li, R.; Xu, L.; Yao, L.; Williams, B.W. Active Control of DC Fault Currents in DC Solid-State Transformers during Ride-Through Operation of Multi-Terminal HVDC Systems. *IEEE Trans. Energy Convers.* **2016**, *31*, 1336–1346. [CrossRef]
11. Peralta, J.; Saad, H.; Dennetiere, S.; Mahseredjian, J.; Nguefeu, S. Detailed and Averaged Models for a 401-Level MMC-HVDC System. *IEEE Trans. Power Deliv.* **2012**, *27*, 1501–1508. [CrossRef]
12. Li, R.; Fletcher, J.; Yao, L.; Williams, B.W. DC fault protection structures at a DC-link node in a radial multi-terminal high-voltage direct current system. *IET Renew. Power Gener.* **2016**, *10*, 744–751. [CrossRef]
13. Li, R.; Xu, D.G. Parallel Operation of Full Power Converters in Permanent-Magnet Direct-Drive Wind Power Generation System. *IEEE Trans. Ind. Electron.* **2013**, *60*, 1619–1629. [CrossRef]
14. Li, R.; Fletcher, J.; Xu, L.; Williams, B. Enhanced Flat-Topped Modulation for MMC Control in HVDC Transmission Systems. *IEEE Trans. Power Deliv.* **2016**. [CrossRef]
15. Jacobson, B.; Karlsson, P.; Asplund, G.; Harnefors, L.; Jonsson, T. VSC-HVDC transmission with cascaded two-level converters. In Proceedings of the 2010 Cigré Session, Paris, France, 22–27 August 2010.
16. Li, B.; Xu, D.; Zhang, Y.; Yang, R.; Wang, G.; Wang, W.; Xu, D. Closed-Loop Precharge Control of Modular Multilevel Converters During Start-Up Processes. *IEEE Trans. Power Electron.* **2015**, *30*, 524–531. [CrossRef]
17. Das, A.; Nademi, H.; Norum, L. A method for charging and discharging capacitors in modular multilevel converter. In Proceedings of the IECON 2011—37th Annual Conference on IEEE Industrial Electronics Society, Melbourne, Australia, 7–10 November 2011; pp. 1058–1062.
18. Li, R.; Xu, L.; Yao, L. DC Fault Detection and Location in Meshed Multi-terminal HVDC Systems Based on DC Reactor Voltage Change Rate. *IEEE Trans. Power Deliv.* **2016**. [CrossRef]